Looking for primordial and intrinsic non-Gaussianity

Robert Crittenden

Institute of Cosmology and Gravitation

University of Portsmouth

ICG Portsmouth

Improving primordial NG constraints with LSS and ISW measurements

Work with **T Giannantonio, A Ross,** W Percival,
D Bacher, B Nichol, M Kilbinger, J Weller

The intrinsic non-Gaussianity of the microwave background

Work with **G Pettinari, C Fidler,** K Koyama, D Wands

ICG Portsmouth

Local non-Gaussianity

I am going to primarily focus on local non-Gaussianity for simplicity, though the constraints can be extended to other types.

In real space: $\Phi(x) = \Phi_G(x) + f_{NL}(\Phi_G^2(x) - \langle \Phi_G^2(x) \rangle)$

Non-Gaussianities are constrained in a variety of ways:

- CMB Bispectrum: Planck $-8 < f_{NL} < 14$
- Abundance of rare objects
- **Scale dependence of large scale bias**
  - Galaxies are known to be biased tracers of the underlying matter density
  - The amount of bias can vary depending on the tracer
  - The degree of biasing is modulated by primordial non-Gaussianity

Non-Gaussianity and structure

The impact of the non-Gaussianity can be seen in simulations of the halos (Dalal et al., 2008.)

$f_{NL} < 0$
less small scale structure in over densities, more in under-densities

$f_{NL} > 0$
more small scale structure in over densities, less in under-densities

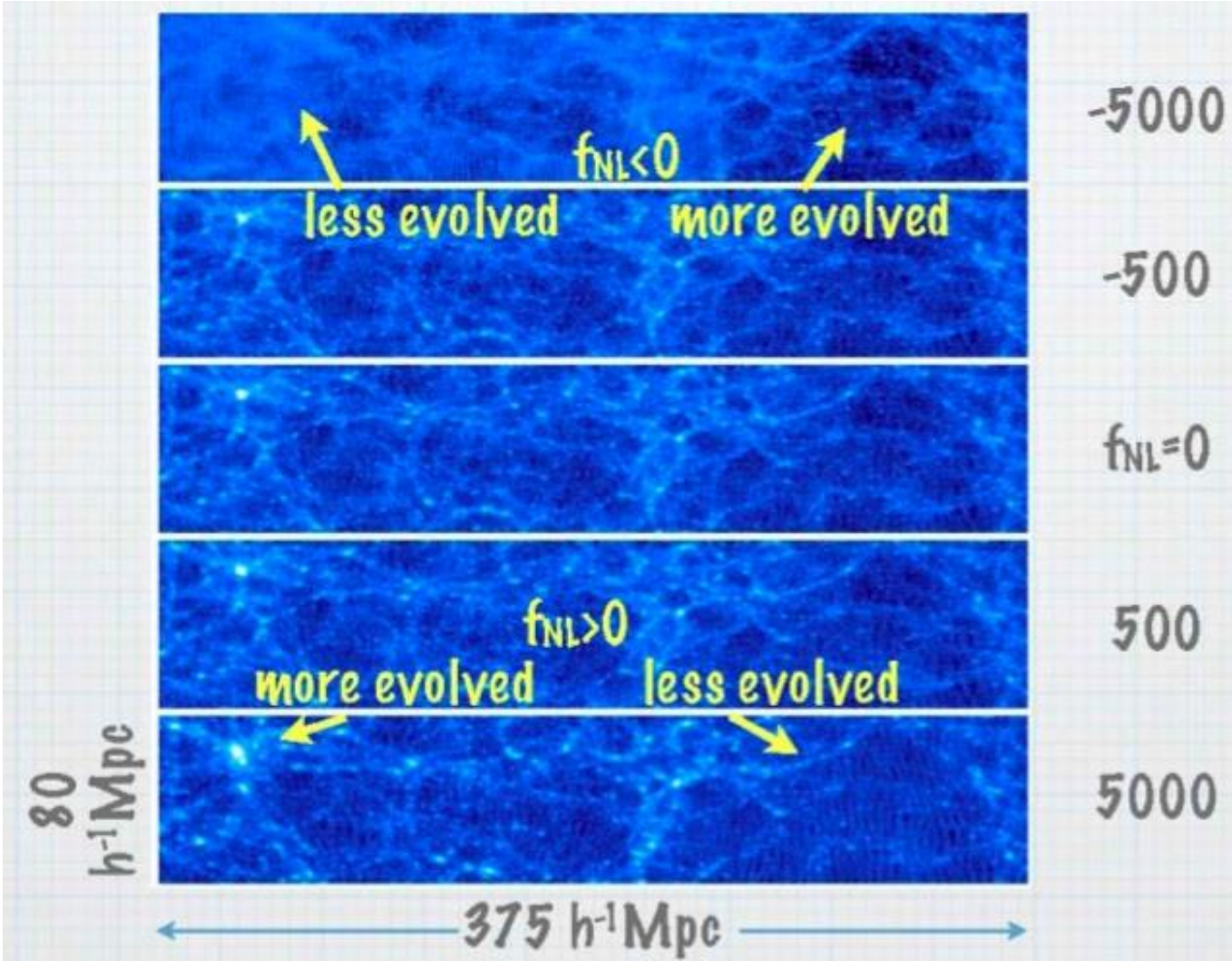

Figure from N Dalal talk

Non-Gaussianity and structure

Non-Gaussianity predicts a scale dependent bias which we can constrain by looking at the power spectrum on large scales.

$$\Delta b(k,z) \propto \frac{b_L f_{NL} \delta_c G \bar{\rho}_m}{k^2 T(k) D(z)}$$

Correction largest for large scales and large f_{NL}

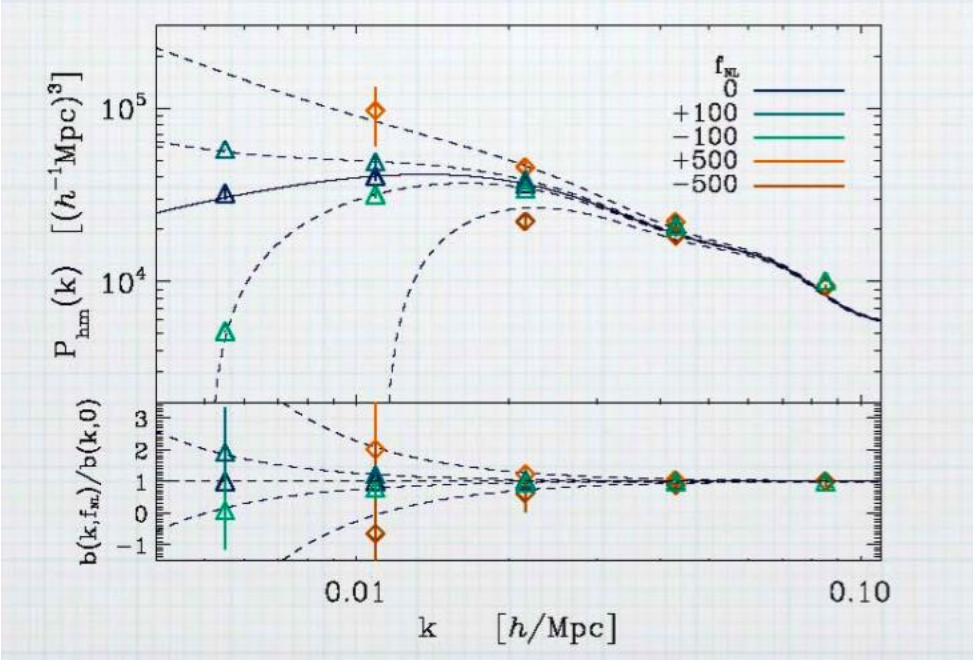

Figure from N Dalal talk

By detecting evidence for large clustering of biased probes on the largest scales, we can try to constrain non-Gaussianity.

Dalal et al 2008, Matarrese & Verde 2008, Slosar et al 2008, Afshordi & Tolley 2008. Desjacques et al 2009, Giannantonio & Porciani 2010, Valageas 2010, …

Previous constraints

Slosar et al (2008)	**QSO, LRG, NVSS-CMB**	**$-29 < f_{NL} < 70$**
Afshordi & Tolley (2008)	**NVSS-CMB**	**$82 < f_{NL} < 390$**
Xia et al (2010)	**NVSS, NVSS-CMB**	**$25 < f_{NL} < 117$**
Xia et al (2010)	**QSO, QSO-CMB**	**$10 < f_{NL} < 106$**
Xia et al (2011)	**NVSS, QSO, MegaZ +**	**$5 < f_{NL} < 84$**
Ross et al (2013)	**BOSS (Spec)**	**$-82 < f_{NL} < 178$**
Planck (2013)	**$-8 < f_{NL} < 14$**	

Systematic issues?

Many of the previous works showed weak evidence for non-Gaussianity and are marginally in disagreement with the Planck results.

Why might have this happened?

One possible culprit is systematics in the measurement of the ACF's.

Small systematics that arise in galaxy surveys can lead to significant problems in the large scale power, where the signal is weakest.

Unfortunately, such systematics have been observed in a number of key surveys used in PNG studies:

- Luminous Red Galaxies (LRGs)
- NVSS radio sources
- SDSS Quasars (QSOs).

LRG systematics

The MegaZ sample from the SDSS saw anomalous structure on large scales, much larger than expected in standard cosmologies (Thomas et al. 2010.)

A more recent careful study of potential systematics by Ross et al (2011) on the BOSS photometric sample found a significant correlation between the densities of galaxies and foreground stars, indicating that stars can make background galaxies harder to detect than was previously supposed.

Correcting for this bias on the new CMASS sample leaves no evidence for the anomalous excess seen in MegaZ.

The resulting WMAP CCF is somewhat lower and more stable to changing the CMB frequency.

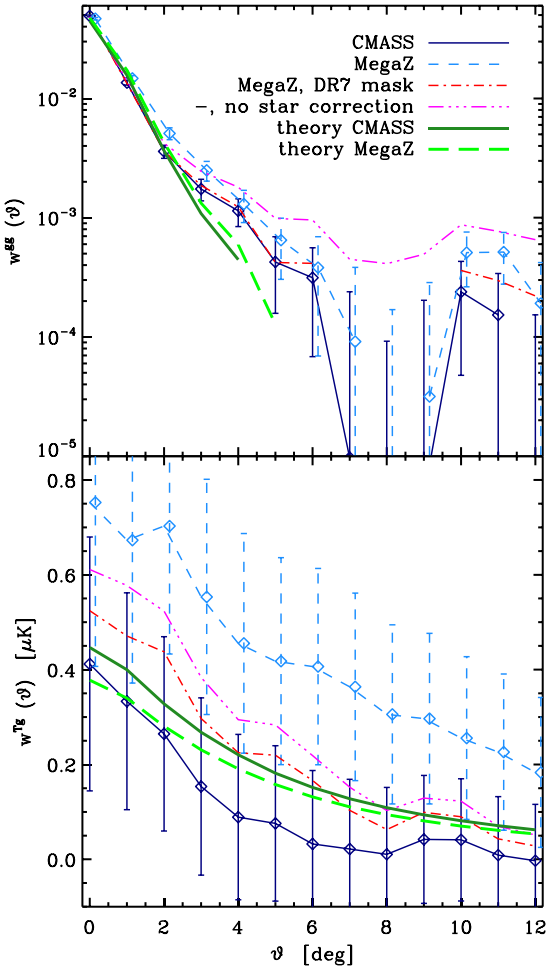

NVSS systematics

The NVSS has a well known (but poorly understood) declination dependent systematic. This has been corrected in various ways:

- Rescaling in bands (Boughn & Crittenden 01)
- Cutting lower flux sources (Blake et al 04)
- Nulling the m=0 modes (Smith et al 07)

For ISW purposes at least, this systematic and the way it is corrected do not make significant changes.

However, there does remain some anomalous power at large scales after this correction.

Recently we have observed a similar, though much smaller, apparent systematic with right ascension, and correcting for it impacts the anomalous power.

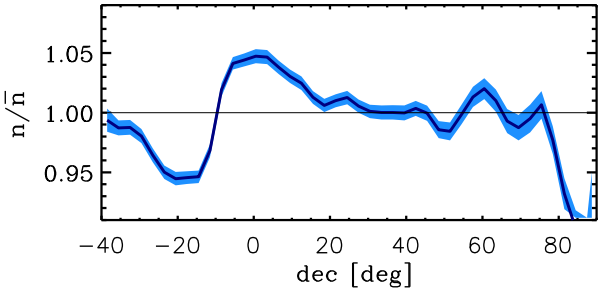

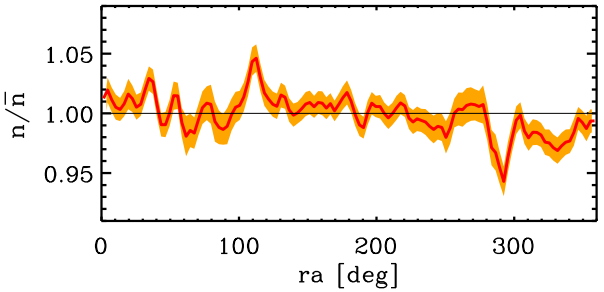

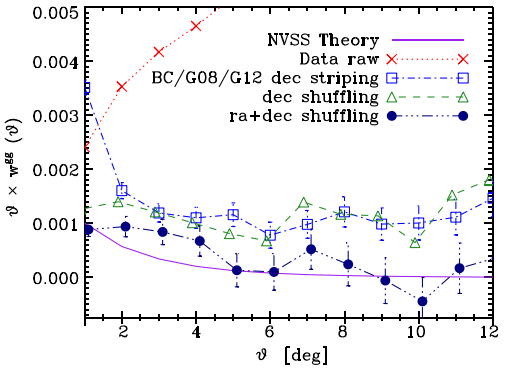

QSO systematics

The SDSS QSO sample is also prone to systematics, not least because it is photometric and is contaminated by stars at the 1% level.

These stars add correlations at large scales and are largely degenerate with the non-Gaussianity signal.

Other issues:

- Unexpected correlations between low and high redshifts (Pullen & Hirata 2012)
- Unstable to splits in photometric redshift and i-band luminosity.
- Related correlations with extinction maps and stellar densities.

Overall, these make the QSO autocorrelations effectively impossible to use to constrain non-Gaussianity. (However, Leistedt et al. (2013)…)

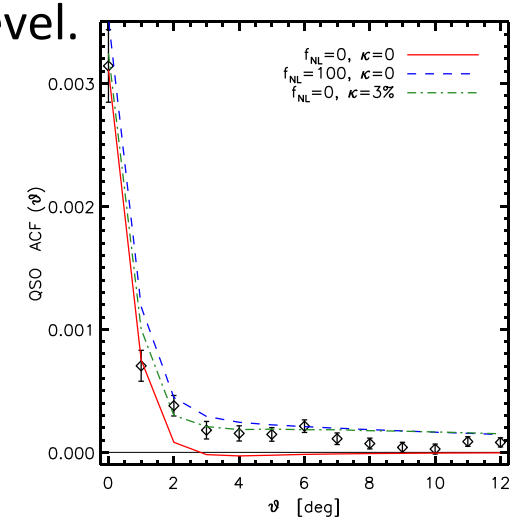

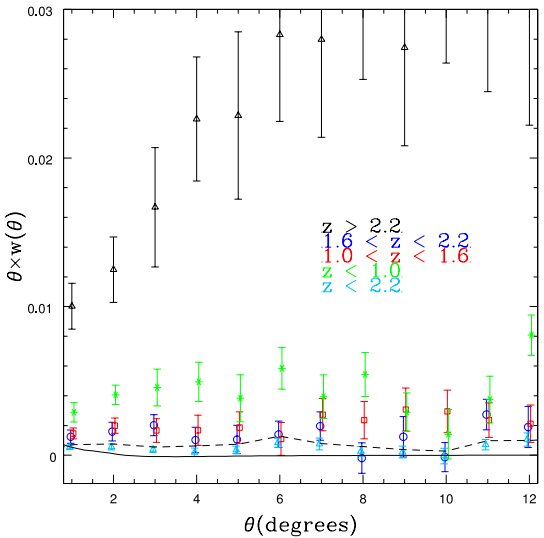

Where else can we look?

If the ACF's are dangerous to look at, how can we gain constraints on primordial non-Gaussianity?

One option is to use the information in cross-correlations between surveys and cross correlations between them and the CMB.

Given six surveys (2MASS, SDSS galaxies, CMASS LRGs, HEAO X-ray background, NVSS, QSO), there are:

- Six auto-correlations
- Six cross correlations with CMB
- Fifteen cross correlations between surveys!

Hopefully any systematics will be uncorrelated between surveys, making them a more reliable but still sensitive probe of the large scale powers.

Not necessarily true for multiple probes based on SDSS (galaxies, LRGs, QSO)!

What to look out for

Great idea in principle, but redshift distributions of objects is uncertain in some of these cases, making the survey overlaps even more uncertain.

For example, Ho et al (2008) used the cross correlations in the reverse way, to infer some of the redshift distributions.

However, many of the distributions are becoming better known; we also marginalize over 15 nuisance amplitudes for the cross correlations, ensuring that it is only their shape which is informing the constraints.

The large scale enhancement signal is distinctive, and ultimately it is the lack of such an enhancement which is providing our limit.

The bias evolution model is also important, and we try to use reasonable bias models consistent with observations.

The quasars are treated differently, as observations suggest their mass is independent of redshift.

$$b_1^i(z) = 1 + \frac{b_0^i - 1}{D^{\gamma_i}(z)}$$

$$b_1^{\rm QSO}(z) = \frac{b_0^{\rm QSO}}{D^{\gamma_{\rm QSO}}(z)}$$

For deep surveys, like NVSS, we also try changing γ.

Our samples

Naïve – Includes all 27 correlations

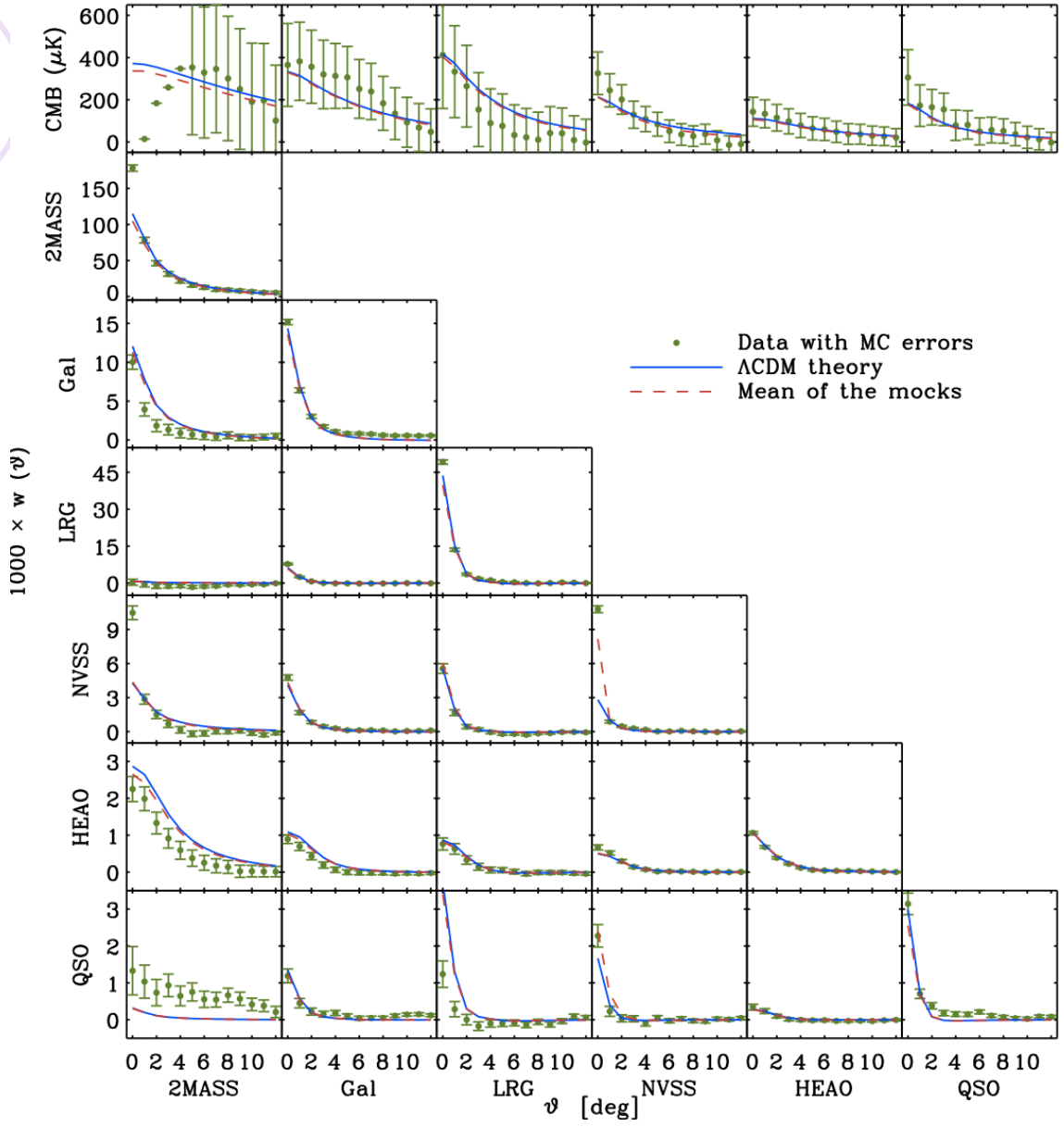

Our samples

Naïve – Includes all 27 correlations

Fair ? – All but two ACF's we know to be potentially unreliable

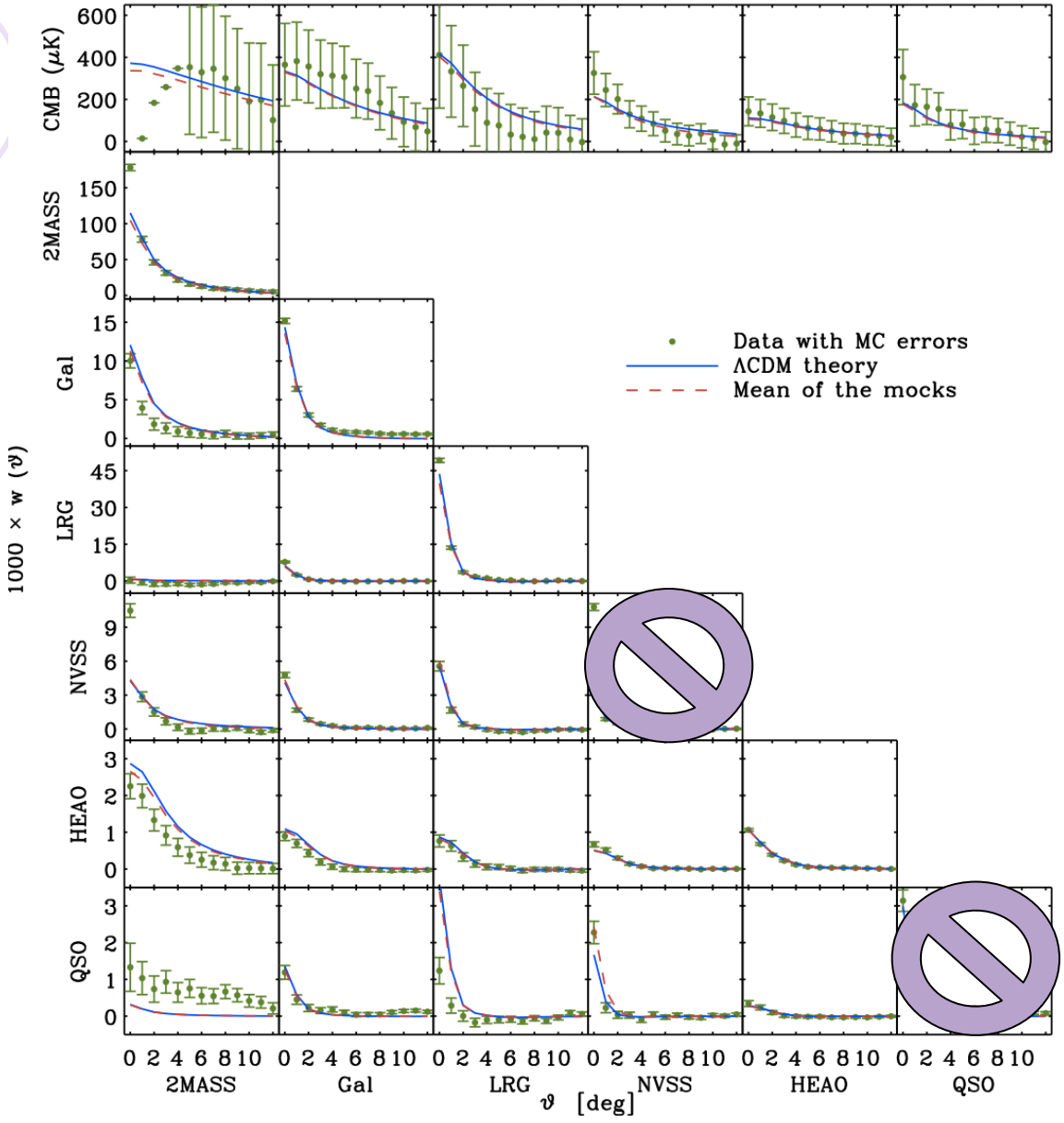

Our samples

Naïve – Includes all 27 correlations

Fair – All but the two ACF's we know to be potentially unreliable

Conservative – Exclude 2MASS and SDSS galaxies entirely, and all ACF's except CMASS, and CMASS-QSO

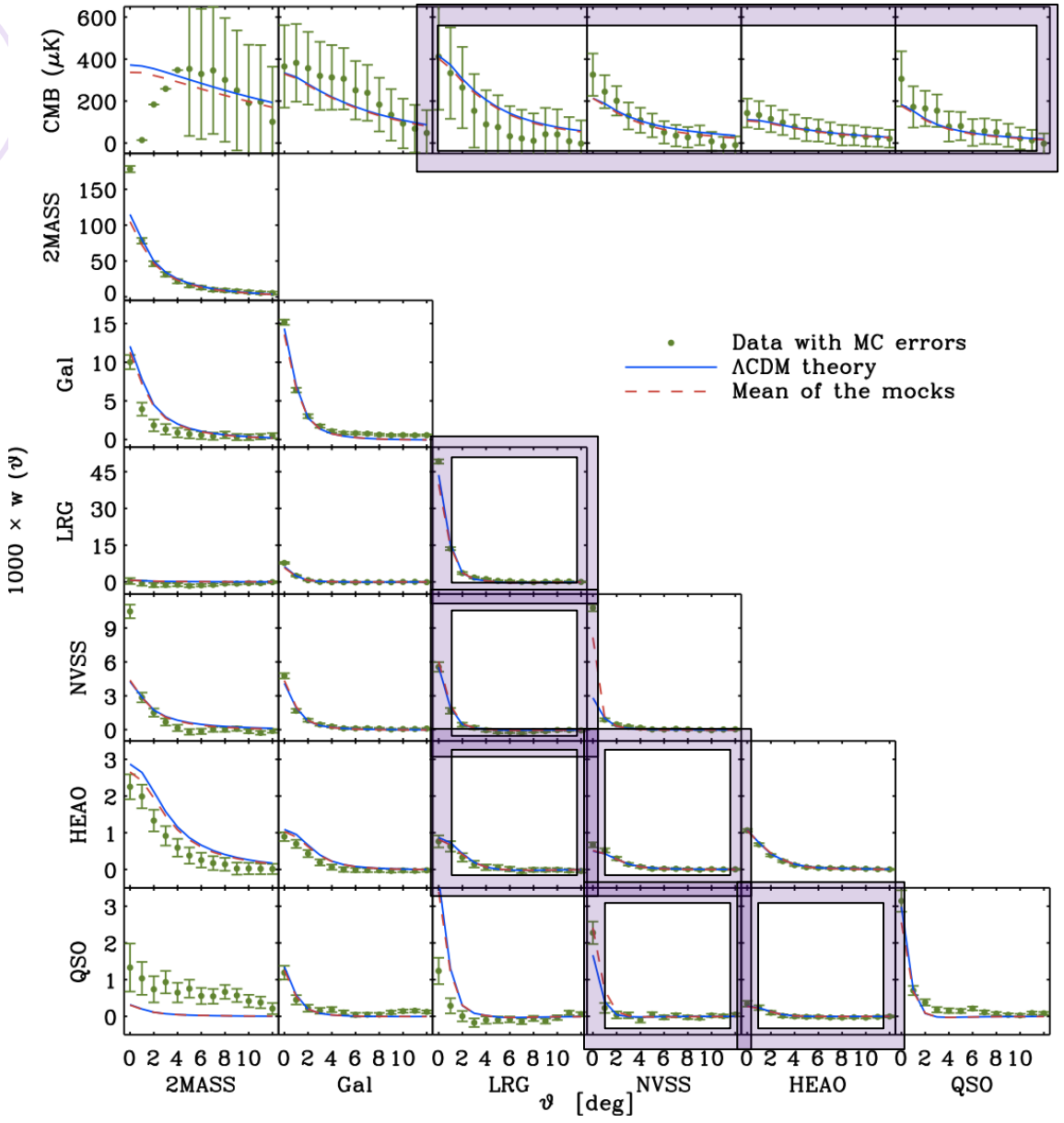

Our results

We calculated the covariance matrices with 10,000 Monte Carlo simulations, marginalised over bias, SDSS stellar contamination and cross amplitudes using multiNest.

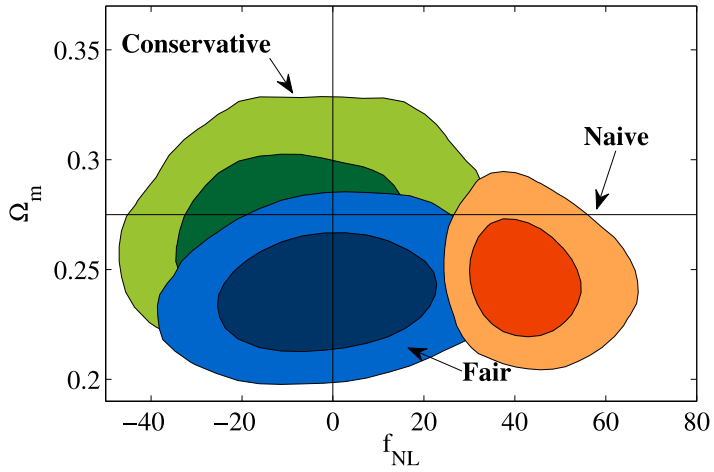

Naïve –

$30 < f_{NL} < 62$ 95% CL

Fair –

$-29 < f_{NL} < 31$ 95% CL

Conservative –

$-37 < f_{NL} < 25$ 95% CL

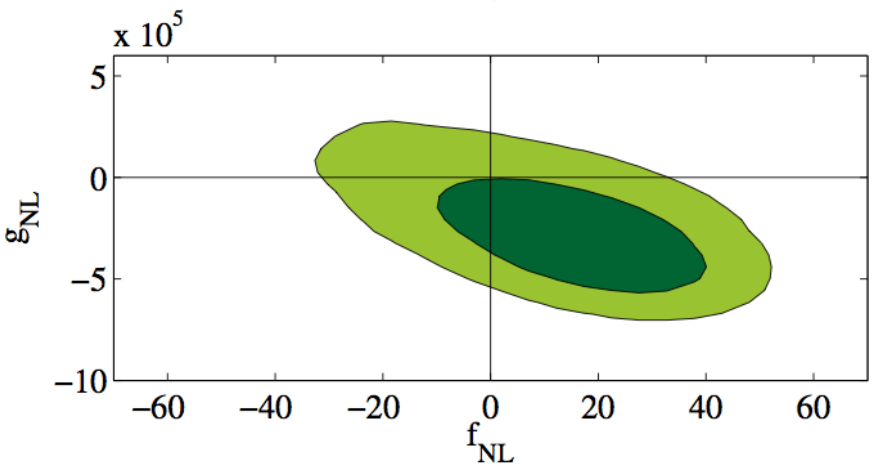

Our results

Weak detection when all data are used, but this appears to be biased by anomalous power in QSO and NVSS.

Excluding these provides a constraint consistent with primordial Gaussianity, and before Planck, it was briefly the strongest constraint!

$$-37 < f_{NL} < 25 \quad 95\%\ CL$$

Luckily, it proved to be consistent with Planck measurement.

Getting ACFs right on large scales is hard, but cross correlations should be less prone to systematics and potentially can provide very strong constraints.

Any questions before shifting topics?

The intrinsic non-Gaussianity of the microwave background

Work with **G Pettinari, C Fidler,** K Koyama, D Wands

ICG Portsmouth

When the CMB gets ~~ugly~~ interesting

We're used to the CMB physics (at least the theory) being very clean and easy to interpret. This is because the perturbations are small (10^{-5}) and a linear treatment becomes a very good approximation.

However, as the measurements improve, we must start worrying whether this approximation is good enough.

When we go beyond the linear analysis, a much richer phenomenology appears even when the initial conditions are simple (scalar, Gaussian):

- Creation of vorticity (vector modes), magnetic fields?
- Gravitational radiation (tensor modes)
- B-modes, spectral distortions
- Intrinsic non-Gaussianity

Non-linearity is expected to generate $f_{NL} \sim 1$, which is close to the Planck sensitivity, so it is essential to understand precisely what it predicts!

The ISW-Lensing signal

Goldberg & Spergel 1999
Seljak and Zaldarriaga 1999
Lewis, Challinor & Hanson 2011
Lewis 2012

Most of the non-Gaussianity Planck has seen is believed to be intrinsic, arising from gravitational lensing and the integrated Sachs-Wolfe effect.

In the ISW effect, large scale over-densities and under-densities appear hotter or colder as photons can gain or lose energy passing through their time dependent potentials. These potentials correlate to where gravitational lensing (seen on smaller scales) is largest or smallest, creating mode coupling.

This can lead to a significant bias in the measurement of f_{NL} of order 7, so it must be subtracted from the Planck signal. It is large because both terms arise along the line of sight, and the perturbations have time to grow non-linear.

The ISW-Lensing signal is generally thought to be the largest contribution to the intrinsic non-Gaussianity, but a systematic treatment is required to to see what other sources may arise.

Linear is easy

As an example, consider the full continuity equation:

$$\frac{\partial \delta}{\partial t} + \nabla_x \cdot \mathbf{v} + \nabla_x \cdot (\mathbf{v}\delta) = 0$$

In the perturbative treatment, we expand $\delta = \delta^{(1)} + \delta^{(2)} + \ldots$ and keep terms of the same order. To linear order, we can drop the last term because its suppressed by 10^{-5} compared to the other terms.

This leads to a simple system which is local in Fourier space, and all the modes decouple. Every mode with the same wavelength evolves in the same way:

$$\Delta \mathrm{T}(\mathbf{k}) \;=\; \Phi(\mathbf{k})\, \mathcal{T}(\mathbf{k})$$

This mode decoupling makes it possible to write codes like CAMB and CLASS which can evolve the Boltzmann equations quickly:

$$C_l \;\propto \int_0^\infty dk\, k^2\, P(k)\, |\, T_l(k)\, |^2$$

Second order is hard

The second order continuity equation becomes

$$\frac{\partial \delta^{(2)}}{\partial t} + \nabla_x \cdot \mathbf{v}^{(2)} + \nabla_x \cdot (\mathbf{v}^{(1)} \delta^{(1)}) = 0$$

where the non-linear terms become sources for the second order perturbations, and are quadratic in the first order terms.

The product in real space is a non-local convolution in Fourier space, coupling all the Fourier modes together.

At second order, the transfer function becomes:

$$\Delta \mathrm{T}(\mathbf{k}) = \mathcal{K}\left[\mathcal{T}(\mathbf{k}, \mathbf{k_1}, \mathbf{k_2})\ \Phi(\mathbf{k_1})\,\Phi(\mathbf{k_2})\right]$$

where $\mathbf{k} + \mathbf{k_1} + \mathbf{k_2} = 0$

This is done on a grid, and means there are many more systems to calculate and much slower codes compared to linear order.

The full calculation

The full system includes the Einstein equations, baryons and dark matter, as well as Boltzmann equations for photons, their polarization and neutrinos. Most of these have non-linear corrections that must be accounted for.

The most important is the Boltzmann equation, which follows how the photon distribution function evolves in time and has many contributions.

$$\frac{\partial f}{\partial \eta} + \frac{dx^i}{d\eta}\frac{\partial f}{\partial x_i} + \frac{dq}{d\eta}\frac{\partial f}{\partial q} + \frac{dn^i}{d\eta}\frac{\partial f}{\partial n_i} = \mathfrak{C}[f]$$

Free streaming

Redshift term
Sachs-Wolfe, ISW

Lensing term
(non-linear)

Scattering term

Each term comes with complex second order source contributions.

Schematic second order Boltzmann

The Boltzmann is usually written in terms of the brightness function, integrating over the photon momentum.

Schematically, this looks like

$$\dot{\Delta}_n + k\Sigma_{nm}\Delta_m + \mathcal{M}_n + \mathcal{Q}_n^L = \mathcal{C}_n$$

Generalised free streaming

Pure metric term Includes quad sources

Mixed quad sources

Scattering term, quad sources

n is shorthand for l, m and polarization, which are coupled together.

Scattering now includes effects like fluctuations in the free electron density.

The mixed sources are the most problematic, including line of sight contributions from time delay, redshift effects and gravitational lensing.

A typical equation

=

$$\frac{1}{k^2}\left(\left(\frac{1}{12}\,\mathbf{k1}^2\,\mathbf{k2}^2\,\mu^4+\frac{1}{24}\,\mathbf{k1}\,\mathbf{k2}^3\,\mu^3+\frac{1}{24}\,\mathbf{k1}^3\,\mathbf{k2}\,\mu^3-\frac{1}{12}\,\mathbf{k1}^2\,\mathbf{k2}^2\,\mu^2-\frac{1}{24}\,\mathbf{k1}\,\mathbf{k2}^3\,\mu-\frac{1}{24}\,\mathbf{k1}^3\,\mathbf{k2}\,\mu\right)h_{(1)}(1)\,h_{(1)}(2)+\right.$$

$$\left(\mathbf{k1}^2\,\mathbf{k2}^2\,\mu^4+\frac{1}{3}\,\mathbf{k1}\,\mathbf{k2}^3\,\mu^3+\frac{1}{2}\,\mathbf{k1}^3\,\mathbf{k2}\,\mu^3-\frac{\mathbf{k2}^4\,\mu^2}{3}-2\,\mathbf{k1}^2\,\mathbf{k2}^2\,\mu^2-2\,\mathbf{k1}\,\mathbf{k2}^3\,\mu-\frac{5}{6}\,\mathbf{k1}^3\,\mathbf{k2}\,\mu-\frac{\mathbf{k2}^4}{3}-\frac{\mathbf{k1}^2\,\mathbf{k2}^2}{3}\right)h_{(1)}(1)\,\eta\mathrm{b}_{(1)}(2)+$$

$$\left(3\,\mathbf{k1}^2\,\mathbf{k2}^2\,\mu^4+\mathbf{k1}\,\mathbf{k2}^3\,\mu^3+\mathbf{k1}^3\,\mathbf{k2}\,\mu^3-\mathbf{k1}^4\,\mu^2-\mathbf{k2}^4\,\mu^2-4\,\mathbf{k1}^2\,\mathbf{k2}^2\,\mu^2-\frac{7}{3}\,\mathbf{k1}\,\mathbf{k2}^3\,\mu-\frac{7}{3}\,\mathbf{k1}^3\,\mathbf{k2}\,\mu+\frac{\mathbf{k1}^4}{3}+\frac{\mathbf{k2}^4}{3}-\frac{\mathbf{k1}^2\,\mathbf{k2}^2}{3}\right)\eta\mathrm{b}_{(1)}(1)\,\eta\mathrm{b}_{(1)}(2)+$$

$$\left(-\mu^2\,e\,a^2-3\,e\,a^2-\frac{2\,\mu\,e\,\mathbf{k2}\,a^2}{\mathbf{k1}}-\frac{2\,\mu\,e\,\mathbf{k1}\,a^2}{\mathbf{k2}}\right)(w+1)\,\theta_{(1)}(1)\,\theta_{(1)}(2)+H\left(\frac{1}{3}\,\mathbf{k1}\,\mathbf{k2}\,\mu^3+\frac{2\,\mathbf{k1}^2\,\mu^2}{3}+\frac{2\,\mathbf{k2}^2\,\mu^2}{3}+\mathbf{k1}\,\mathbf{k2}\,\mu\right)h_{(1)}(1)\,h_{(1)}{}'(2)+$$

$$H\left(2\,\mathbf{k1}\,\mathbf{k2}\,\mu^3+2\,\mathbf{k1}^2\,\mu^2+4\,\mathbf{k2}^2\,\mu^2+\frac{10\,\mathbf{k1}\,\mathbf{k2}\,\mu}{3}+\frac{2\,\mathbf{k1}^2}{3}-\frac{4\,\mathbf{k2}^2}{3}\right)\eta\mathrm{b}_{(1)}(1)\,h_{(1)}{}'(2)+\left(\frac{1}{6}\,\mathbf{k1}\,\mathbf{k2}\,\mu^3+\frac{5\,\mathbf{k1}^2\,\mu^2}{24}+\frac{5\,\mathbf{k2}^2\,\mu^2}{24}+\frac{\mathbf{k1}\,\mathbf{k2}\,\mu}{6}-\frac{\mathbf{k1}^2}{24}-\frac{\mathbf{k2}^2}{24}\right)h_{(1)}{}'(1)\,h_{(1)}{}'(2)+$$

$$H\left(2\,\mathbf{k1}\,\mathbf{k2}\,\mu^3+4\,\mathbf{k1}^2\,\mu^2+2\,\mathbf{k2}^2\,\mu^2+\frac{10\,\mathbf{k1}\,\mathbf{k2}\,\mu}{3}-\frac{4\,\mathbf{k1}^2}{3}+\frac{2\,\mathbf{k2}^2}{3}\right)h_{(1)}(1)\,\eta\mathrm{b}_{(1)}{}'(2)+H\left(12\,\mathbf{k1}\,\mathbf{k2}\,\mu^3+12\,\mathbf{k1}^2\,\mu^2+12\,\mathbf{k2}^2\,\mu^2+4\,\mathbf{k1}\,\mathbf{k2}\,\mu-4\,\mathbf{k1}^2-4\,\mathbf{k2}^2\right)\eta\mathrm{b}_{(1)}(1)\,\eta\mathrm{b}_{(1)}{}'(2)+$$

$$\left(2\,\mathbf{k1}\,\mathbf{k2}\,\mu^3+\frac{5\,\mathbf{k1}^2\,\mu^2}{2}+2\,\mathbf{k2}^2\,\mu^2+\frac{4\,\mathbf{k1}\,\mathbf{k2}\,\mu}{3}-\frac{5\,\mathbf{k1}^2}{6}-\frac{\mathbf{k2}^2}{3}\right)h_{(1)}{}'(1)\,\eta\mathrm{b}_{(1)}{}'(2)+\left(6\,\mathbf{k1}\,\mathbf{k2}\,\mu^3+6\,\mathbf{k1}^2\,\mu^2+6\,\mathbf{k2}^2\,\mu^2+2\,\mathbf{k1}\,\mathbf{k2}\,\mu-2\,\mathbf{k1}^2-2\,\mathbf{k2}^2\right)\eta\mathrm{b}_{(1)}{}'(1)\,\eta\mathrm{b}_{(1)}{}'(2)+$$

$$\left(\frac{1}{6}\,\mathbf{k1}\,\mathbf{k2}\,\mu^3+\frac{\mathbf{k1}^2\,\mu^2}{3}+\frac{\mathbf{k2}^2\,\mu^2}{3}+\frac{\mathbf{k1}\,\mathbf{k2}\,\mu}{2}\right)h_{(1)}(1)\,h_{(1)}{}''(2)+\left(\mathbf{k1}\,\mathbf{k2}\,\mu^3+\mathbf{k1}^2\,\mu^2+2\,\mathbf{k2}^2\,\mu^2+\frac{5\,\mathbf{k1}\,\mathbf{k2}\,\mu}{3}+\frac{\mathbf{k1}^2}{3}-\frac{2\,\mathbf{k2}^2}{3}\right)\eta\mathrm{b}_{(1)}(1)\,h_{(1)}{}''(2)+$$

$$\left.\left(\mathbf{k1}\,\mathbf{k2}\,\mu^3+2\,\mathbf{k1}^2\,\mu^2+\mathbf{k2}^2\,\mu^2+\frac{5\,\mathbf{k1}\,\mathbf{k2}\,\mu}{3}-\frac{2\,\mathbf{k1}^2}{3}+\frac{\mathbf{k2}^2}{3}\right)h_{(1)}(1)\,\eta\mathrm{b}_{(1)}{}''(2)+\left(6\,\mathbf{k1}\,\mathbf{k2}\,\mu^3+6\,\mathbf{k1}^2\,\mu^2+6\,\mathbf{k2}^2\,\mu^2+2\,\mathbf{k1}\,\mathbf{k2}\,\mu-2\,\mathbf{k1}^2-2\,\mathbf{k2}^2\right)\eta\mathrm{b}_{(1)}(1)\,\eta\mathrm{b}_{(1)}{}''(2)\right)$$

Synchronous gauge, checked against Tomita, 1967

Bispectrum from second order physics

Integrating these equations leads to the second order transfer functions.

The leading order bispectrum combines two first order transfer functions with one of the second order ones.

$$b_{l_1 l_2 l_3} = \int dr\, r^2 \int dk_1\, k_1^2\, T_{l_1}(k_1)\, P(k_1)\, j_{l_1}(r\, k_1) \int dk_2\, k_2^2\, T_{l_2}(k_2)\, P(k_2)\, j_{l_2}(r\, k_2) \int dk_3\, k_3^2\, T_{l_3}(k_1, k_2, k_3)\, j_{l_3}(r\, k_3)$$

Second-order transfer function

Its not practical to calculate every possible triangular configuration, so we end up having to interpolate on a grid for these calculations.

Laying the groundwork

Most earlier approximations either neglect part of the source terms or focus on a particular configuration.

Approximation	Reference	f_{NL} contamination
Super horizon scales	Bartolo et al. 2004 Boubekeur et al. 2009	~ 1
Small angular scales	Pitrou et al. 2008	$O(10)$
Perturbed recombination	Senatore et al. 2009 Khatri et al. 2009	- 3.5 / - 1
Only quadratic sources	Nitta et al. 2009	+ 1
Full computation 'CMBQuick' Mathematica	Pitrou et al. 2010	+ 5
Squeezed limit	Lewis 2012 Bartolo et al. 2011 Creminelli et al. 2011	negligible for $L_{LONG} < 100$

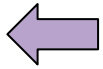

Analytic results

An analytical approximation can be made in the squeezed limit, where one mode is outside the horizon at recombination. Through means of a coordinate transformation, the large scale mode is seen to change the observed angular size of smaller modes.

$$b_{\ell_1\ell_2\ell_3} = -C_{\ell_1}^{T\zeta}\frac{1}{2}\left(C_{\ell_2}\frac{d\ln\left(l_2^2\,C_{\ell_2}\right)}{d\ln l_2} + C_{\ell_3}\frac{d\ln\left(l_3^2\,C_{\ell_3}\right)}{d\ln l_3}\right)$$

Combining this with other effects from lensing, a fuller analytic approximation was derived:

Creminelli et al. 2011
Bartolo et al. 2011
Lewis 2012

$$b_{l_L l_S l_S} = C_{l_L}\,C_{l_S}(1+6\cos 2\theta)\left(2 - \frac{d\ln(l_S^2 C_{l_S})}{d\ln l_S}\right)$$

These predict $|f_{NL}| < 1$ in tension with CMBQuick results.

Rising to the challenge

To resolve this issue, a number of groups have been working to develop accurate and faster second order Boltzmann codes, building on the **CMBQuick** work by Pitrou et al. (2010):

- Huang & Vernizzi – Full sky Boltzmann code **CosmoLib2nd**, (see talk later today.)
- Su, Lim & Shellard - Flat sky Boltzmann code (Shellard talk Friday?)
- Our group, led by Guido Pettinari and Christian Fidler, has developed a full sky code called **SONG** (Second Order Non-Gaussianity) building on the **CLASS** first order code.

Given the complexity of the problem, its very helpful to have these independent efforts, often using quite different methods and approximations, to check for errors and convergence.

Things to get right

The calculations themselves have many independent pieces, all of which must be carefully checked and optimized for speed:

- Derivation of equations
- Implementation of differential system
- Line of sight integration
- Calculation of bispectrum
- Calculation of bispectrum estimators and their signal-to-noise.

Line of sight terms

Terms on the surface of last scattering are relatively straightforward, but there are also a number of terms along the line of sight, like lensing, which are not. These are potentially large and entangled with the surface terms.

Huang & Vernizzi (2012) showed that some of these sources, which take a particular form (a product of a first order source times the first order distribution function) could be accounted for by a change of variables.

Such line of sight terms seem to account for the difference between the squeezed calculations and Pitrou et al. (2010). The extra term partially cancels a larger signal from recombination (Pettinari et al., (2013).)

However, this is only part of the story, as other contributions such as lensing are still not included. Ideally, since these could be correlated, all contributions should be treated in a single calculation.

Bispectrum comparison

Previous numerical calculations (Pitrou et al 2010) ignored some line of sight effects which appear to cancel some of the signal!

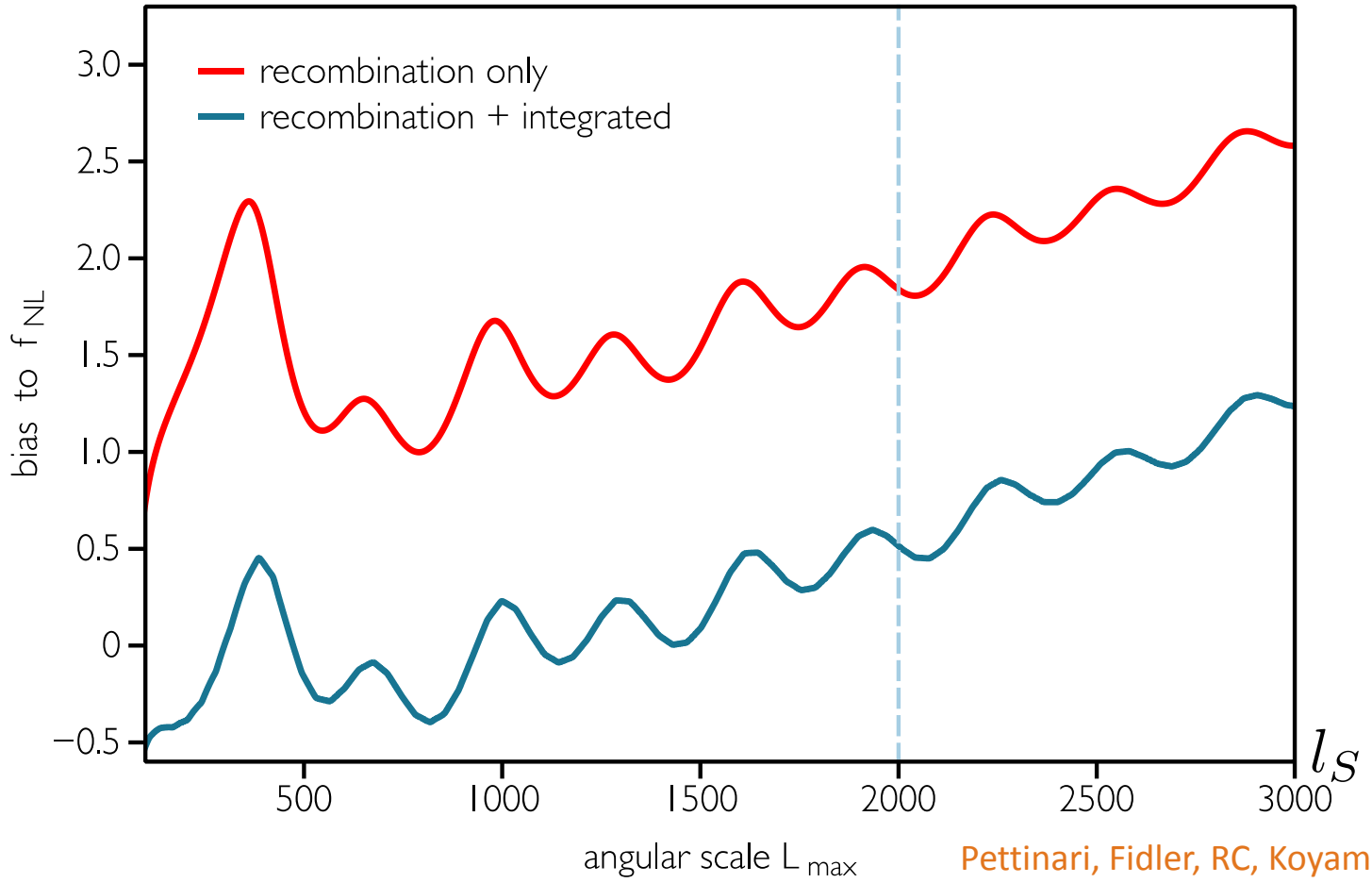

Pettinari, Fidler, RC, Koyama, Wands
arXiv:1302.0832

Detecting the intrinsic signal

Even using the perfect template, it would be hard to see the intrinsic signal with Planck.

Signal-to-noise ratio

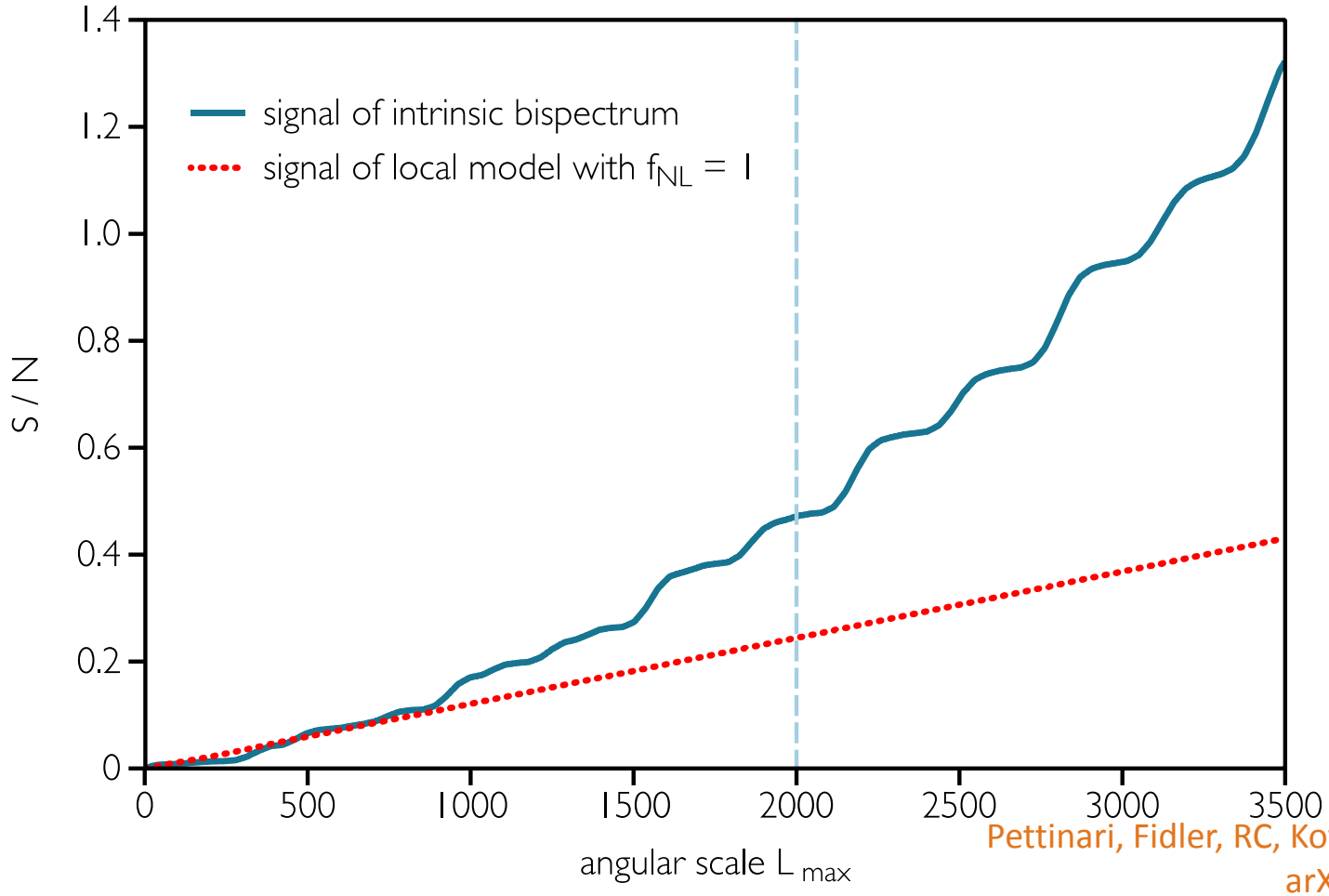

Pettinari, Fidler, RC, Koyama, Wands
arXiv:1302.0832

Much to be done

Tremendous progress has been made, and indications are that the other intrinsic non-Gaussianity sources are just beyond the Planck sensitivity.

There is still much work to be done:

- More cross checking of results from different codes
- Including vector and tensor contributions, potentially important for non-squeezed configurations
- Including polarization into the non-Gaussian estimators
- Including all line-of-sight contributions coherently, including the ISW-lensing term at second order
- Checking the calculations in synchronous gauge

Tune in to talks by Zhiqi and Guido!

The CMB physics

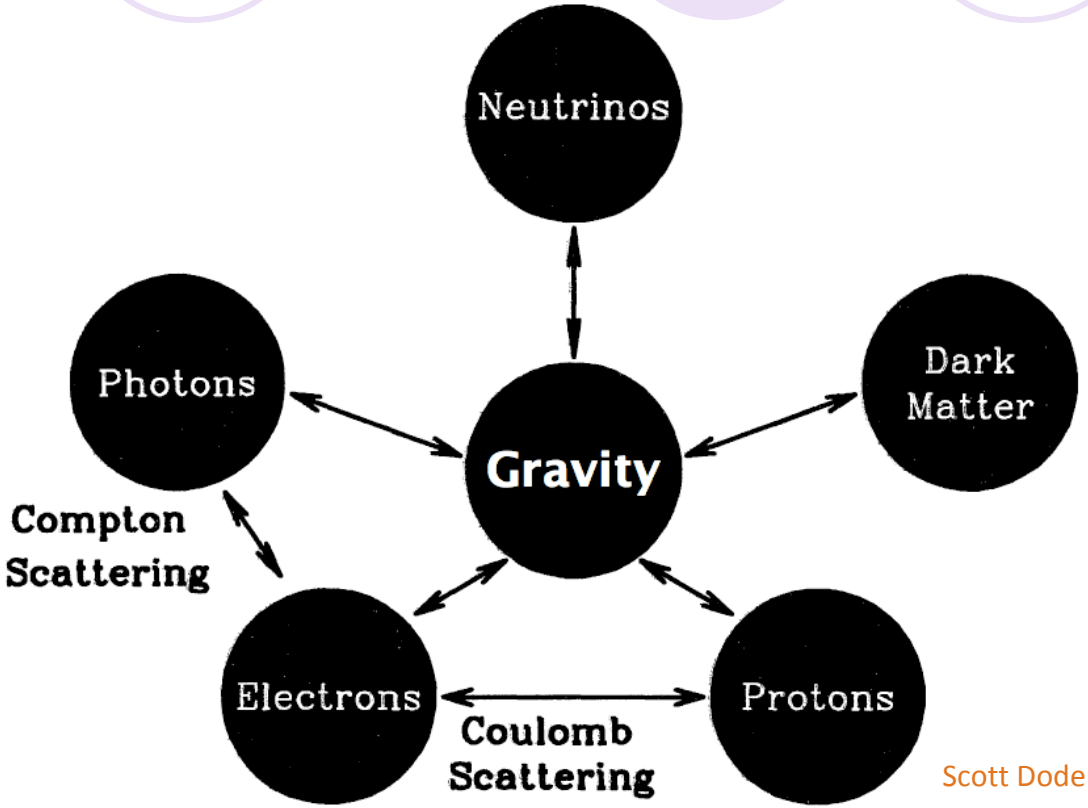

Scott Dodelson, Modern Cosmology

The dominant physics arises from acoustic oscillations of the photon-baryon fluid, which ends when the electrons and protons combine to form hydrogen.

The CMB power spectrum

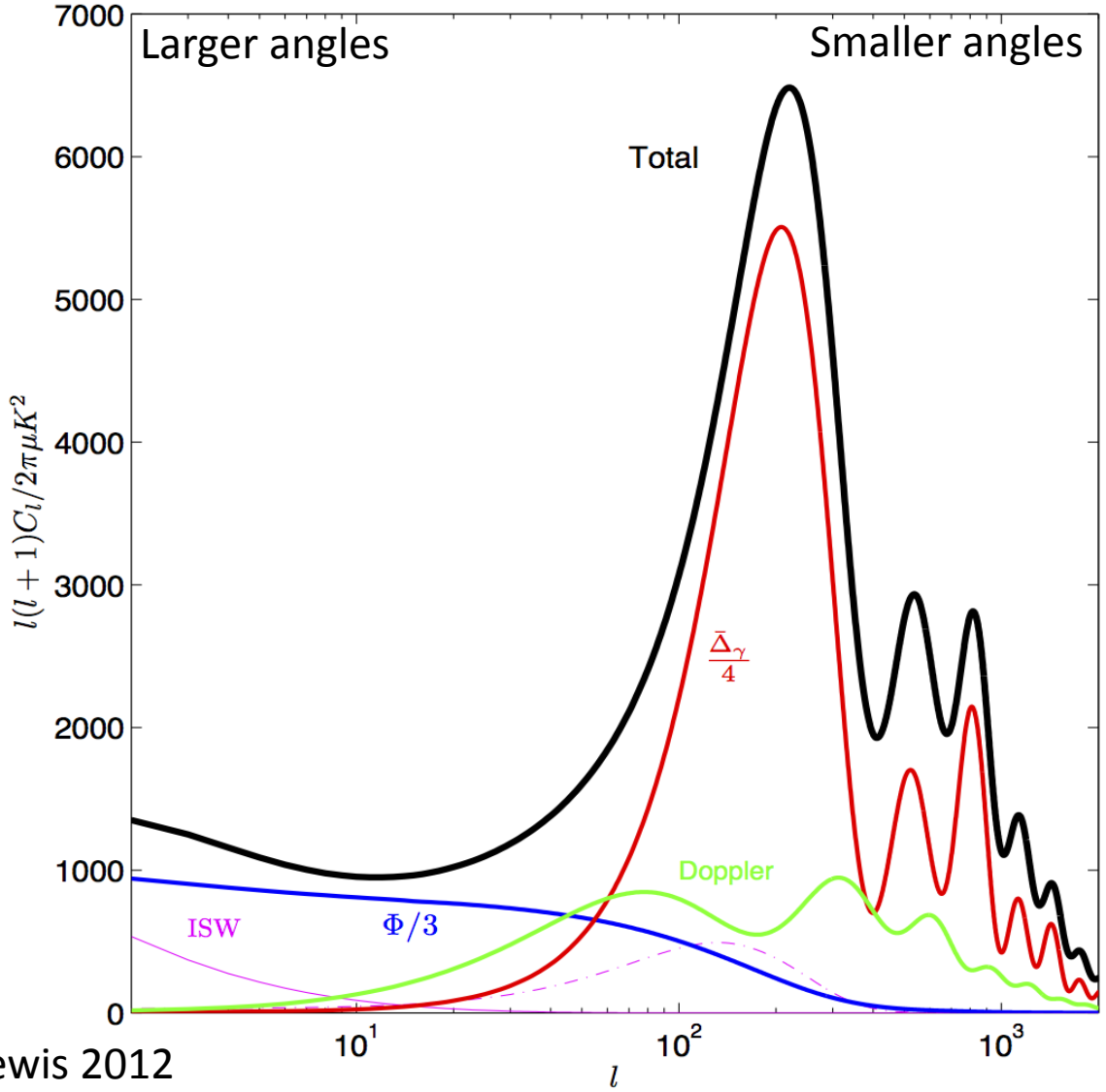

Lewis 2012

Oscillations in the photon density captured at a single time.

Doppler effect from scattering off moving electrons.

Photons must climb out of gravitational wells on the last scattering surface (Sachs-Wolfe).

Gravitational line-of-sight effect from evolving potentials (iSW).

Intrinsic non-Gaussianity?

As our limits get stronger, we need to reconsider our assumption that the late time processes are purely linear in nature.

We may need to factor in the non-linear physics which can make maps non-Gaussian even if the seeds themselves are Gaussian.

Kinds of effects I will be discussing: non-linear gravitational clustering and scattering effects, primarily at recombination.

What I won't discuss in detail: CMB foregrounds and observing systematics, and other non-linear astrophysics that potentially create non-Gaussianity through rescattering.

CMB foregrounds

The CMB measurements are also contaminated by a range of non-Gaussian foreground sources, which usually have different frequency dependences.

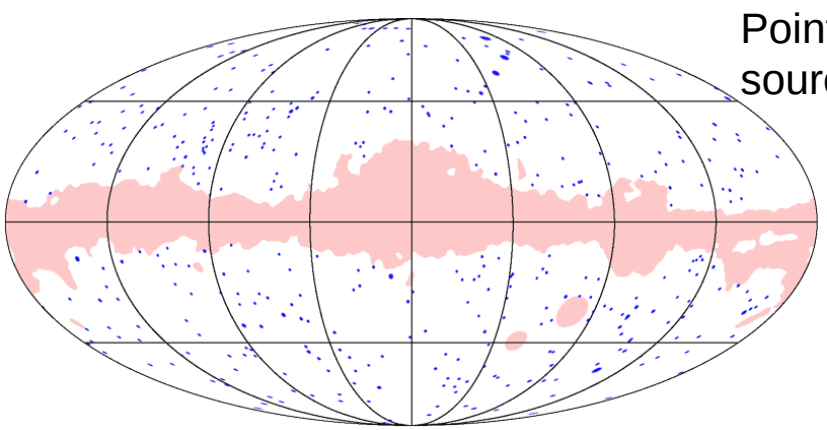

Point sources

Dust

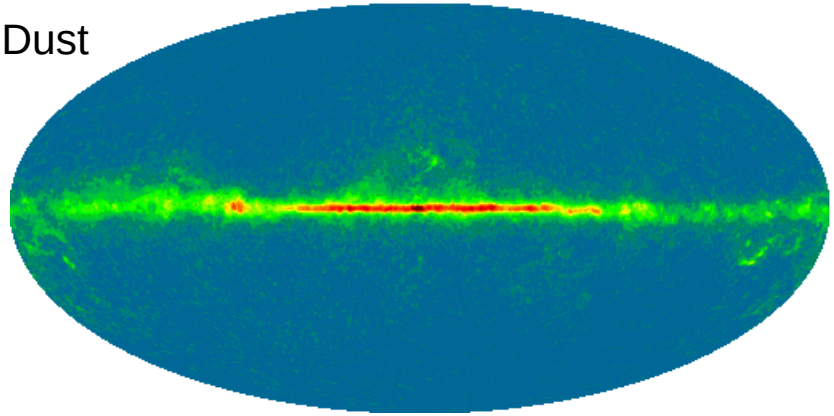

Free-free

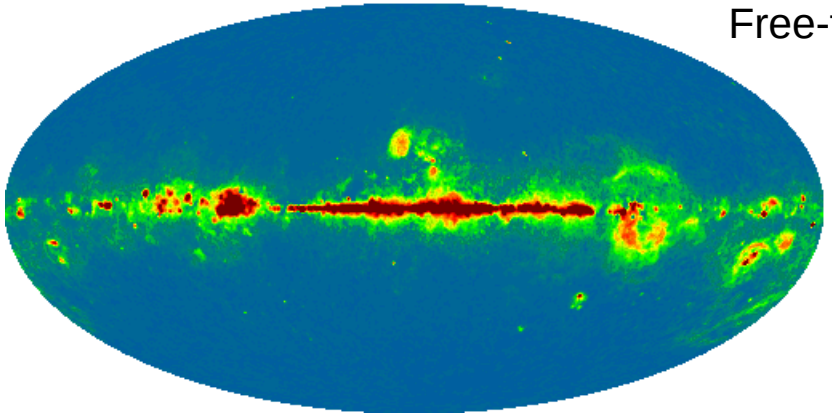

Synchrotron

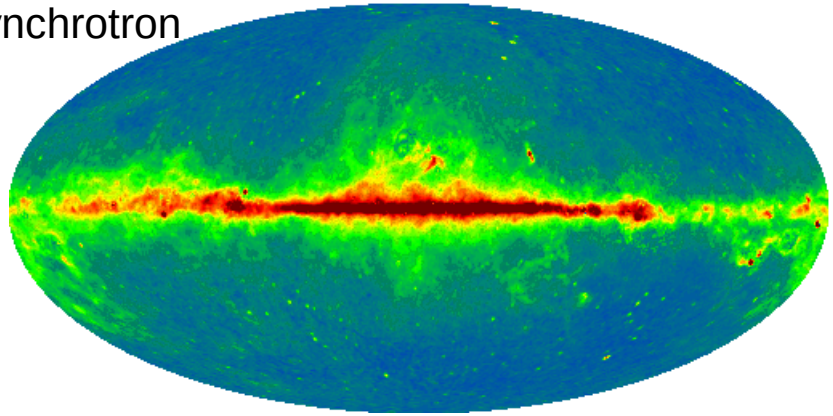

Patchy reionisation and the SZ effect

At some point the first stars create radiation which ionizes the hydrogen in the Universe, allowing it to scatter CMB photons.

The non-instantaneous percolation of these regions leads to variation in the amount of scattering and could potentially introduce non-Gaussianity on small scales.

The Sunyaev-Zeldovich effect, where CMB photons are upscattered by hot gas in clusters, can also produce non-Gaussianity.

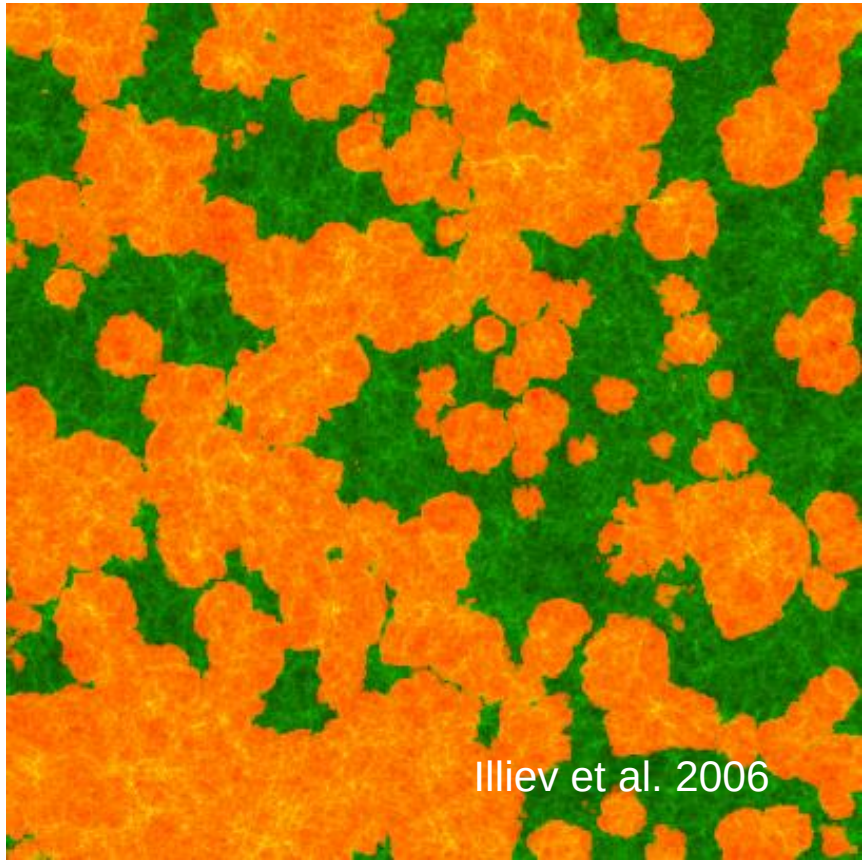

Bispectrum comparison

Comparison of our results with analytical results in squeezed limit

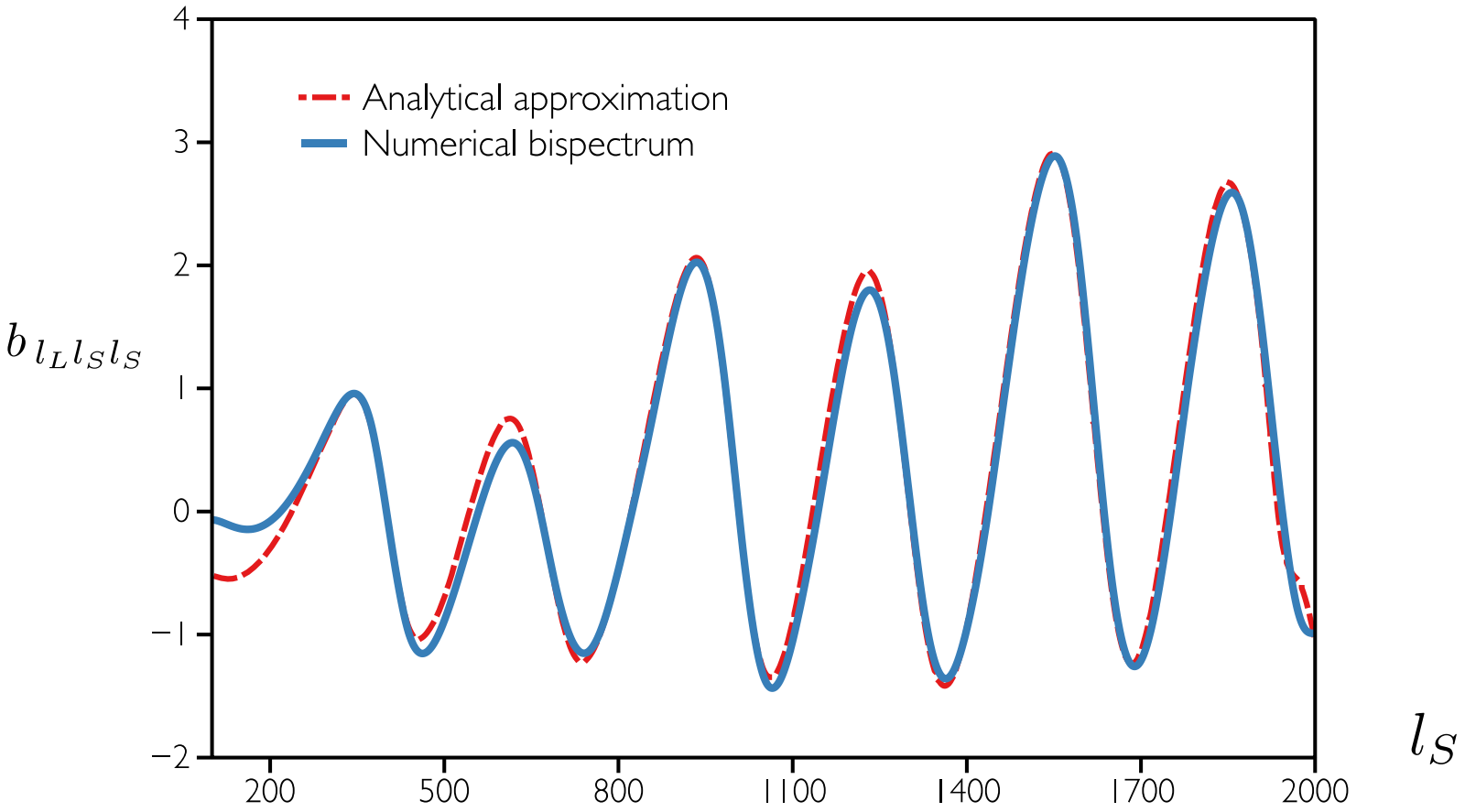

Pettinari, Fidler, RC, Koyama, Wands
arXiv:1302.0832

Bias on local non-Gaussianity

Luckily, the bias will be small compared to Planck sensitivity

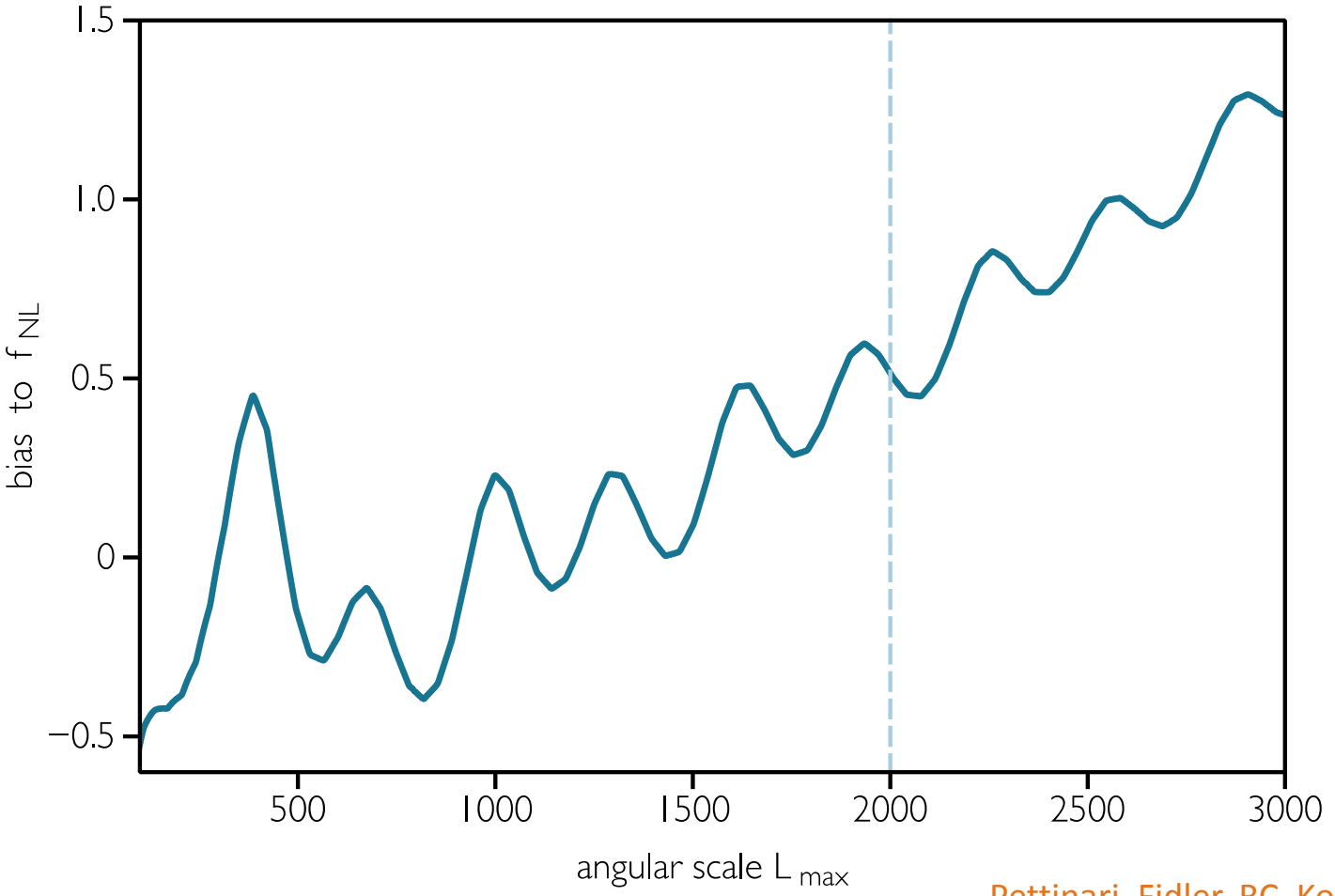

Pettinari, Fidler, RC, Koyama, Wands
arXiv:1302.0832

Second order B modes

The B-mode polarisation will not contaminate the primordial signal unless the tensor to scalar ratio is lower than $r \sim 10^{-4}$

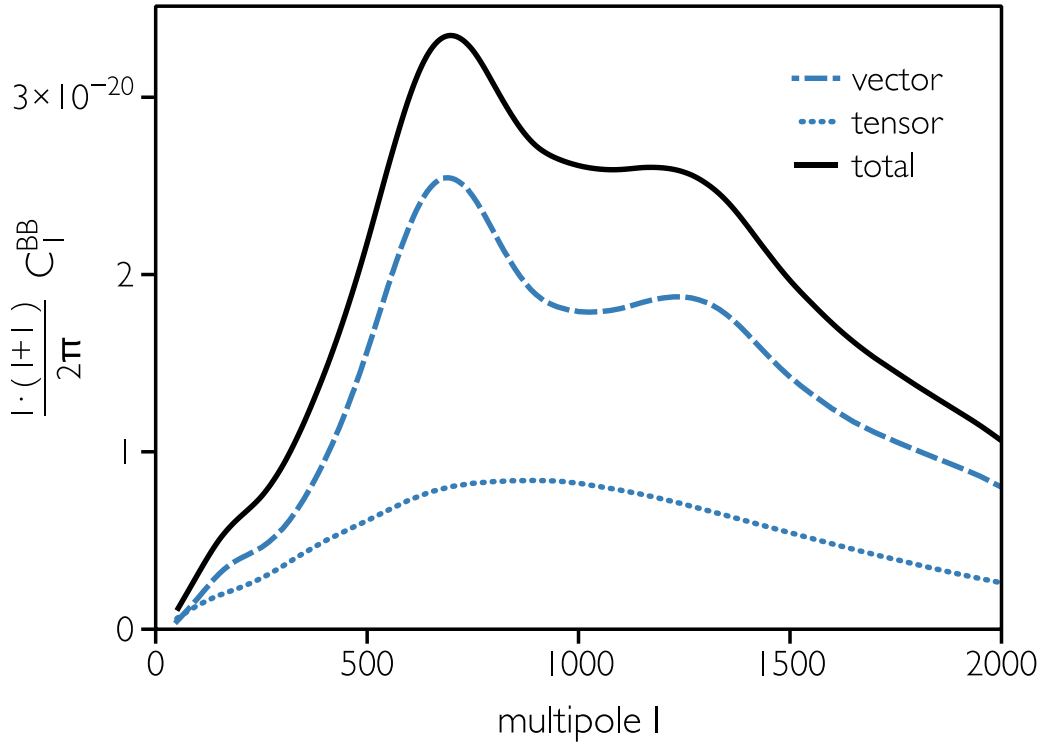

To be submitted in 2013, Fidler C, Pettinari, G, RC, Koyama K, Wands D.

Non-Gaussianity and structure

Non-Gaussianity can affect the distribution of structure on large scales, giving rise to a scale-dependent bias.

Bias and the peak-background split

We actually observe discrete objects (halos) which form at rare peaks of the density field.

The criterion for their formation is assumed to depend only on local physics, such as the density exceeding a critical threshold.

Where these form is affected by large scale density fluctuations, which can push more peaks above the threshold.

How the number of peaks responds to the large scale background density defines the bias:

$$n(\mathbf{x}) = \bar{n}(1 + b_L \delta_l(\mathbf{x}))$$

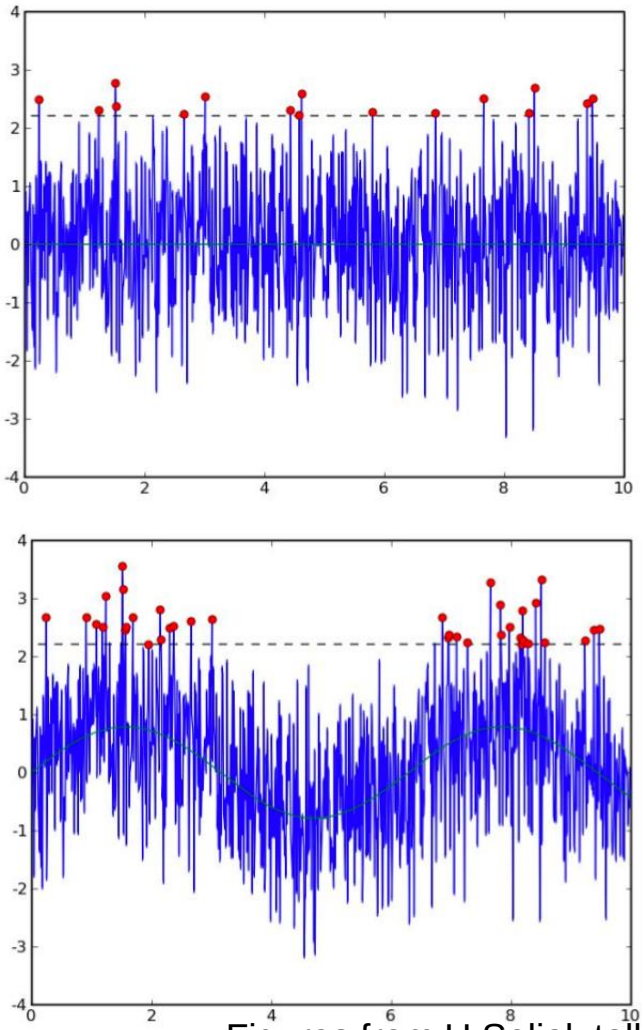

Figures from U Seljak talk

Non-Gaussianity and structure

Non-Gaussianity can affect the distribution of structure on large scales, giving rise to a scale-dependent bias.

Effect of non-Gaussianity

In non-Gaussian models, there is another factor which can affect the number of halos. Recall that the amount of small scale power is not uniform, but is modulated slightly by the large scale modes:

$$\delta(\mathbf{x}) \simeq \delta_G(\mathbf{x}) + 2 f_{NL} \Phi_G^l(\mathbf{x}) \delta_{\mathbf{G}}(\mathbf{x})$$

In the usual picture, the small scale power is the same everywhere, but here the amount of small scale power depends on the large scale gravitational potential.

After smoothing over small scales, the fluctuation in the number of halos is affected by both factors:

$$\delta_h(\mathbf{x}) = b_L(\delta_l(\mathbf{x}) + 2 f_{NL} \Phi_G^l(\mathbf{x}) \delta_c)$$

Non-Gaussianity and structure

Non-Gaussianity can affect the distribution of structure on large scales, giving rise to a scale-dependent bias.

Scale dependent bias

$$\delta_h(\mathbf{x}) = b_L(\delta_l(\mathbf{x}) + 2f_{NL}\Phi^l_G(\mathbf{x})\delta_c)$$

The number of halos depends on the large scale density and the initial large scale gravitational potential, which themselves are related via the Poisson equation, which in Fourier space looks like:

$$-k^2\Phi^l(\mathbf{k}, t_i) = 4\pi G\bar{\rho}_m(t_i)\delta_l(\mathbf{k}, t_i)$$
$$\delta_l(\mathbf{x}, t) = T(k)D(t, t_i)\delta_l(\mathbf{k}, t_i)$$

Where the latter use the density transfer function and the growth factor. Factoring out the density from the second term, one infers a scale dependent correction to the bias,

$$\Delta b(k, z) \propto \frac{b_L f_{NL}\delta_c G\bar{\rho}_m}{k^2 T(k)D(z)}$$